PHILOSOPHICAL TRANSACTIONS OF THE ROYAL SOCIETY A

rsta.royalsocietypublishing.org

Research

Cite this article: Saha S, Majumdar R, Hussain A, Dighe RR, Chakravarty AR. 2013 Biotin-conjugated tumour-targeting photocytotoxic iron(III) complexes. Phil Trans R Soc A 371: 20120190.
http://dx.doi.org/10.1098/rsta.2012.0190

One contribution of 18 to a Discussion Meeting Issue 'Photoactivatable metal complexes: from theory to applications in biotechnology and medicine'.

Subject Areas:
inorganic chemistry

Keywords:
iron, dipyridophenazine biotin conjugates, streptavidin binding, photocytotoxicity, cellular uptake, reactive oxygen species

Author for correspondence:
Akhil R. Chakravarty
e-mail: arc@ipc.iisc.ernet.in

Electronic supplementary material is available at http://dx.doi.org/10.1098/rsta.2012.0190 or via http://rsta.royalsocietypublishing.org.

Royal Society Publishing
Informing the science of the future

Biotin-conjugated tumour-targeting photocytotoxic iron(III) complexes

Sounik Saha[1], Ritankar Majumdar[2], Akhtar Hussain[1], Rajan R. Dighe[2] and Akhil R. Chakravarty[1]

[1]Department of Inorganic and Physical Chemistry, and [2]Department of Molecular Reproduction, Development and Genetics, Indian Institute of Science, Bangalore 560012, India

Iron(III) complexes [FeL(B)] (**1**–**4**) of a tetradentate phenolate-based ligand (H_3L) and biotin-conjugated dipyridophenazine bases (B), *viz.* 7-aminodipyrido [3,2-*a*:2′,3′-*c*]-phenazine (dppza in **1**), (*N*-dipyrido[3,2-*a*:2′,3′-*c*]-phenazino)amidobiotin (dppzNB in **2**), dipyrido [3,2-*a*:2′,3′-*c*]-phenazine-11-carboxylic acid (dppzc in **3**) and 2-((2-biotinamido)ethyl) amidodipyrido[3,2-*a*:2′,3′-*c*]-phenazine (dppzCB in **4**) are prepared, characterized and their interaction with streptavidin and DNA and their photocytotoxicity and cellular uptake in various cells studied. The high-spin iron(III) complexes display Fe(III)/Fe(II) redox couple near −0.7 V versus saturated calomel electrode in dimethyl sulfoxide–0.1 M tetrabutylammonium perchlorate. The complexes show non-specific interaction with DNA as determined from the binding studies. Complexes with appended biotin moiety show similar binding to streptavidin as that of free biotin, suggesting biotin conjugation to dppz does not cause any loss in its binding affinity to streptavidin. The photocytotoxicity of the complexes is tested in HepG2, HeLa and HEK293 cell lines. Complex **2** shows higher photocytotoxicity in HepG2 cells than in HeLa or HEK293, forming reactive oxygen species. This effect is attributed to the presence of overexpressed sodium-dependent multi-vitamin transporters in HepG2 cells. Microscopic studies in HepG2 cells show internalization of the biotin complexes **2** and **4** essentially occurring by receptor-mediated endocytosis, which is similar to that of native biotin and biotin fluorescein isothiocyanate conjugate.

1. Introduction

Photodynamic therapy (PDT) is a relatively new therapeutic method for the treatment of malignant and non-malignant tumours. PDT involves selective activation of a photosensitizing drug with light of a suitable wavelength. Although selective photo-irradiation of a porphyrin-based photodrug generates cytotoxic reactive oxygen species (ROS) in the tumour, severe skin sensitivity has been reported for the US Food and Drug Administration approved drug Photofrin [1,2]. It has thus become necessary to develop tumour-specific delivery agents for chemotherapeutic and PDT agents that can recognize the intrinsic differences between the normal and tumour cells. In general, a tumour-targeting drug delivery system (DDS) consists of a tumour recognition moiety and a cytotoxic or photocytotoxic agent connected directly or through a suitable linker to form a conjugate [3]. The tumour-targeting DDS should have bio-essential constituents that are systemically non-toxic prior to activation. Moreover, the linker unit must be stable in blood circulation, but upon internalization into the tumour cells, the conjugate may become cleaved to release the cytotoxic or PDT agent.

Cancer cells overexpress many tumour-specific receptors, which can be used as biomarkers to deliver cytotoxic agents into tumours [4]. Monoclonal antibodies [5–8], polyunsaturated fatty acids [9,10], folic acid [11–13], aptamers [14,15], transferrin [16], oligopeptides [17] and hyaluronic acid [18] have widely been used as tumour-specific agents to design tumour-targeting drug conjugates. Although vitamins are essential to all living organisms for their existence, rapidly dividing cancer cells require certain vitamins to sustain their rapid growth [19,20]. Therefore, the receptors involved in uptake of the vitamins are overexpressed on the cancer cell surface. These vitamin receptors serve as useful biomarkers for the imaging and identification of tumour cells as well as tumour-targeted drug delivery. Vitamin B_{12}, folic acid, biotin and riboflavin as the essential vitamins for cell division are particularly important for the growth of tumours. The folate receptors have been recognized as potentially excellent targeting agents, and there has been significant research development in this area [21–23]. In contrast, the biotin receptors have not been investigated in detail for this purpose [24]. Recently, highly specific targeting of a second-generation taxoid in leukaemia cells has been achieved by conjugation of the drug to biotin through a self-immolative linker [24]. Biotin (vitamin H or B_7) as a growth promoter at the cellular level acts as a cofactor for a wide range of carboxylases and hence is required in relatively larger quantities in tumours than in normal tissues. It has been reported that the biotin receptors (sodium-dependent multi-vitamin transporters; SMVTs) are overexpressed more than any other vitamin receptors in various cancer cell types [19,20].

Our recent work has shown that through suitable modification of the phenazine moiety in the ternary iron(III) complexes of dipyridophenazine ligand, the DNA photocleavage activity and photocytotoxicity of the complexes can be highly modulated [25,26]. The 7-aminodppz (dppza) and dppz-11-carboxylic acid (dppzc) complexes of iron(III) present an opportunity for suitable conjugation of cancer cell targeting molecules such as biotin and folic acid. In the present work, we have conjugated biotin to the dipyridophenazine base with an objective to target specifically the photocytotoxic iron(III) complexes to tumours. The uptake of biotin by the cells is known to occur through the SMVTs and mono-carboxylate transporters. The SMVTs are overexpressed in most cancer cells and are excellent biomarkers for tumour-targeted drug design. Herein, we report new ternary iron(III) complexes [Fe^{III}L(B)] (**1**–**4**) using dipyridophenazine derivatives (B) with or without a biotin moiety, *viz.* 7-aminodipyrido[3,2-*a*:2′,3′-*c*]-phenazine (dppza in **1**), (*N*-dipyrido[3,2-*a*:2′,3′-*c*]-phenazino)amidobiotin (dppzNB in **2**), dipyrido[3,2-*a*:2′,3′-*c*]phenazine-11-carboxylic acid (dppzc in **3**) and 2-((2-biotinamido)ethyl)amidodipyrido[3,2-*a*:2′,3′-*c*]-phenazine (dppzCB in **4**) (scheme 1). This work describes unprecedented *in vitro* photosensitizing activity of the targeted iron(III)-based photocytotoxins. The complexes are also investigated for their DNA and streptavidin-binding affinity, as substrates, for proteases and photocytotoxicity in HepG2, HeLa and HEK293 cells. Cellular uptake of the complexes has been monitored by staining with streptavidin–fluorescein isothiocyanate (FITC) conjugate which showed an endocytotic mode of uptake of the biotin-conjugated complexes. The significant results of this work include the

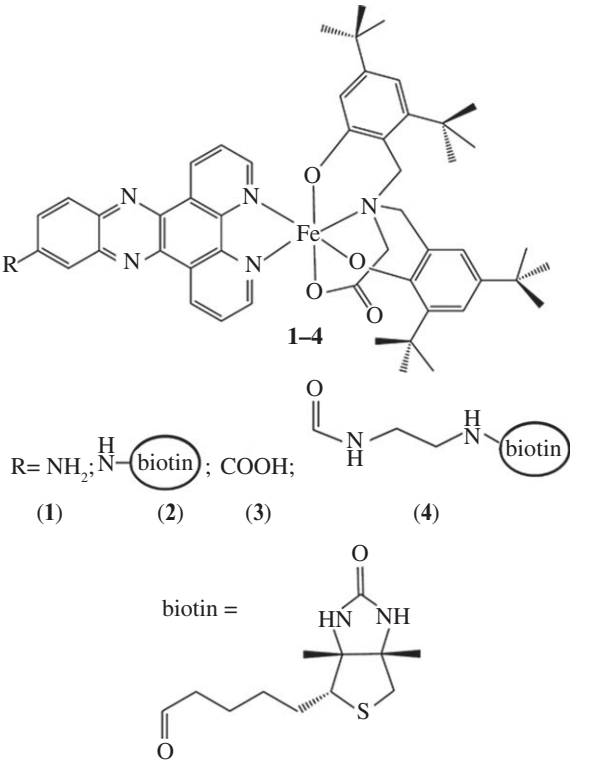

Scheme 1. Schematic drawing of the complexes and the ligands used.

retention of streptavidin-binding ability of the biotin complexes **2** and **4**, indicating that these molecules can also target the SMVTs. Low dark toxicity and enhanced photocytotoxicity in liver hepatocellular HepG2 cells over cervical HeLa cells and human embryonic kidney HEK293 cells are observed for the amidobiotin complex **2**.

2. Experimental

(a) Material and measurements

The reagents and chemicals were procured from commercial sources (Sigma-Aldrich, USA; s.d. Fine Chemicals, India) and used as received without any further purification. The solvents used were purified by standard procedures [27]. Calf thymus (ct) DNA, proteinase K, streptavidin, 4′-hydroxyazobenzene-2-carboxylic acid (HABA), 3-[4,5-dimethylthiazol-2-yl]-2,5-diphenyltetrazolium bromide (MTT), 2′,7′-dichlorodihydrofluorescein diacetate (DCFH-DA) and ethidium bromide (EB) were from Sigma-Aldrich (USA). Tris(hydroxymethyl)aminomethane–HCl (Tris–HCl) buffer was prepared using deionized and sonicated triple distilled water. The ligand H_3L was prepared using a literature method that was modified by carrying out a one-pot Mannich reaction of glycine with two equivalents of 2,6-di-*tert*-butylphenol in the presence of two equivalents of paraformaldehyde in an acetic acid medium [28]. Complexes **1** and **3** were prepared by published procedures [26]. The preparative procedures and characterization data for the dppz bases, *viz.* biotinylethylenediamine, dppzCB, biotin-conjugated fluorescein isothiocynate (BFITC) and dppzNB are given in the electronic supplementary material. The cell lines HepG2 (CRL-1074) and HEK293 (CRL-1573) were from the American Type Culture Collection and the HeLa cells were from the National Center for Cell Science, Pune, India.

The elemental analysis was carried out using a Thermo Finnigan FLASH EA 1112 CHNS analyzer. The infrared and electronic spectra were recorded on Bruker Alpha Fourier transform

infrared (FT-IR) and PerkinElmer Lambda 650 spectrophotometers, respectively. Magnetic susceptibilities of the dimethyl sulfoxide (DMSO) solutions of the complexes at 25°C were measured by the nuclear magnetic resonance (NMR) method, using 4 per cent tetramethylsilane (TMS) as the internal reference [29]. The magnetic moments were calculated by the Evans method using the equation $\mu_{\text{eff}} = 0.0618(\Delta fT/fM)$, where Δf is the change in shift in frequency of the TMS signal, T is the temperature (in K), f is the oscillator frequency (in MHz) and M is the molarity of the complex [30]. Molar conductivity measurements were carried out using a Control Dynamics (India) conductivity meter. Cyclic voltammetric measurements were made at 25°C using an EG&G PAR 253 VersaStat potentiostat/galvanostat with a three-electrode configuration consisting of a glassy carbon working electrode, a platinum wire auxiliary and a saturated calomel reference (SCE) electrode. Ferrocene ($E_f = 0.42$ V) was used as a standard in MeCN–0.1 M [Bu^n_4N](ClO_4) (tetrabutylammonium perchlorate; TBAP). Electrospray ionization mass and ^{1}H NMR spectral measurements were made using Esquire 300 Plus ESI Model (Bruker Daltonics) and Bruker 400 MHz NMR spectrometers, respectively.

(b) Synthesis of [FeL(B)] (B = dppzNB in **2** and dppzCB in **4**)

The iron(III) complexes were prepared by a general preparative procedure in which the ligand H_3L (0.127 g, 0.25 mmol) taken in a mixture of MeOH, EtOH and MeCN (3:3:2 v/v, 20 ml) was reacted with Et_3N (0.1 ml, 0.75 mmol) followed by addition of $Fe(NO_3)_3 \cdot 9H_2O$ (0.102 g, 0.25 mmol). The solution was stirred for 15 min followed by addition of the dipyridophenazine base (B = 0.129 g, dppzNB; 0.147 g, dppzCB). The solution was filtered after 10 min. The filtrate upon slow evaporation gave a dark purple solid.

[FeL(dppzNB)] (**2**): Yield, 40% (0.108 g). Anal. Calc. for $C_{60}H_{71}FeN_8O_6S$: C 66.23; H, 6.58; N, 10.30. Found: C, 66.00; H, 6.80; N, 10.09%. Inductively coupled plasma optical emission spectrometry (ICP-OES): Calc. %Fe: 5.13; Found %Fe: 5.15. Molar conductance in *N*,*N*-dimethylformamide (DMF) ($\Lambda_M/\text{Sm}^2\,\text{mol}^{-1}$): 15. FT-IR (KBr phase): 2954vs, 1698m, 1647vs, 1625vs, 1470s, 1441s, 1412s, 1357s, 1300m, 1265s, 1241s, 1173m, 1120w, 1013m, 837m, 738w, 609w, 520m, 484w, 408m cm^{-1} (vs, very strong; s, strong; m, medium; w, weak). Electrospray ionization mass spectrometry (ESI-MS) in MeOH (m/z): 1088.5 $(M + H)^+$. UV–Vis in 6% DMF/Tris–HCl buffer [λ_{max}/nm ($\varepsilon/\text{dm}^3\,\text{mol}^{-1}\,\text{cm}^{-1}$)]: 468 (8770), 307 (29 790), 273 (35 670). μ_{eff} (298K): 5.95 μ_B.

[FeL(dppzCB)] (**4**): Yield, 47% (0.115 g). Anal. Calc. for $C_{63}H_{76}FeN_9O_7S$: C 65.27; H, 6.61; N, 10.87; Found: C, 64.92; H, 6.52; N, 10.73%. ICP-OES: Calc. %Fe: 4.82; Found %Fe: 4.81. $\Lambda_M/\text{S}\,\text{m}^2\,\text{mol}^{-1}$ in DMF: 19. FT-IR (KBr phase): 3249w, 3129m, 2954vs, 1705s, 1649s, 1605s, 1436m, 1389s, 1360m, 1324m, 1266m, 1063s, 834s, 737s, 660m, 617s, 541s, 469m, 405m cm^{-1}. ESI-MS in MeOH (m/z): 1159.6 $(M + H)^+$. UV–Vis in 6% DMF/Tris–HCl buffer [λ_{max}/nm ($\varepsilon/\text{dm}^3\,\text{mol}^{-1}\,\text{cm}^{-1}$)]: 480 (5850), 385 (19 080), 367 (20 800), 272 (80 900). μ_{eff} (298K): 6.01 μ_B.

The complexes were soluble in CH_2Cl_2, MeOH, EtOH, MeCN, DMF and DMSO. The complexes were stable in the solution phase.

(c) 4′-Hydroxyazobenzene-2-carboxylic acid assay

HABA assay was carried out by a reported protocol [31]. Briefly, aliquots (5 µL) of biotin, complexes **2** and **4** (550 µM) in methanol were added cumulatively to a mixture of avidin (3.8 µM) and HABA (0.3 mM) in potassium phosphate buffer (2 ml, 50 mM, pH 7.4) at 1.0 min intervals. The binding of the complexes to avidin was indicated by a decrease of the absorbance at 500 nm owing to the displacement of HABA from the avidin by the complexes. The binding stoichiometries of the complexes to avidin were determined from a plot of $-\Delta A_{500\,\text{nm}}$ versus [compound]:[avidin].

(d) DNA-binding experiments

The DNA-binding experiments were carried out in Tris–HCl/NaCl buffer (5 mM Tris–HCl, 5 mM NaCl, pH 7.2) or phosphate buffer pH 7.4 using the DMF solution of complexes **2** and **4** using procedures reported previously [25,32–34].

(e) Proteinase K assay

Proteinase K (10 mg) was dissolved in 1.0 ml of water and diluted to 1 : 1000 with water prior to use. To a 2.5 ml (6% DMF/50 mM Tris–HCl buffer, pH 7.4) solution of the ligand dppzNB or dppzCB (1 mM) was added 0.5 ml of proteinase K solution (1 : 1000 diluted). The reaction mixture was incubated at 37°C for 4 h in the dark. The reaction was stopped by additon of 2 ml of trichloroacetic acid–acetone mixture (1 : 1 v/v) to precipitate the enzyme, and the supernatants were transferred to separate vials. The supernatants were then analysed by ESI-MS. As control, similar experiments were carried out with the ligands, but without proteinase K treatment.

(f) Cell cytotoxicity experiments

Photocytotoxicity studies on the iron(III) complexes **1–4** were carried out in HepG2, HeLa and HEK293 cells and the cell viability was measured by the MTT assay [35,36]. Briefly, 1.2×10^4 HepG2, 0.8×10^4 HeLa or 2×10^4 HEK293 cells were plated into the wells of a 96-well tissue culture plate and were cultured for 24 h in a CO_2 incubator with Dulbecco's modified eagle medium (DMEM)/10 per cent fetal bovine serum (FBS) until it reached 70 per cent confluency. Different concentrations of the complex dissolved in 1 per cent DMSO were then added to the wells in triplicate. After the required incubation period, the contents of the plate were discarded and phosphate buffered saline (PBS) was added to it and photoexposed to visible light (400–700 nm) using a Luzchem Photoreactor (Model LZC-1, Ontario, Canada) fitted with Sylvania fluorescent white tubes with a fluence rate of 2.4 mW cm^{-2} to provide a light dose of 10 J cm^{-2}. The PBS was replaced with fresh media and incubation was carried out for 24 h in the dark. The cells for dark controls were kept in PBS for the same length of time as the cells that were exposed to light to exclude any potential effects of autophagy. Thereafter, a 20 µL quantity of the MTT solution (stock concentration: 5 mg ml^{-1}) was added to each well, and plates were incubated at 37°C for 3 h, which resulted in the optimal conditions to evaluate the cell viability. The resulting purple formazan crystals were dissolved on addition of DMSO and the absorbance was read in a BioRad plate reader. To ensure that all experiments were performed in the linear range of the assay, initial standardization assays were carried out. The IC_{50} values were determined by nonlinear regression analysis using GraphPad Prism v. 5.0.

(g) Cellular internalization

Internalization of biotin (10 nM), BFITC (10nM) and the complexes **2** and **4** (20 µM) were studied by treating HepG2 or HEK293 cells with the complexes for 3 and 12 h in a CO_2 incubator at 37°C in the dark. After the required incubation period, the treatment was removed and the cells were washed twice thoroughly with PBS (pH 7.4). For confocal microscopic visualization, the treated cells were fixed in 4 per cent paraformaldehyde in PBS for 30 min at 4°C and then permeabilized for 5 min with 0.1 per cent triton X-100 in PBS followed by washing the cells twice with PBS. To reduce non-specific binding of the streptavidin–FITC conjugate, the cells were treated with blocking buffer (PBS containing 10% FBS) and incubated for 20 min at 25°C. Cells were incubated with streptavidin–FITC (Sigma-Aldrich; 4 µg ml^{-1}, according to manufacturer's protocol) in PBS with 2 per cent FBS for 1 h. The cells treated with BFITC did not require any staining with streptavidin–FITC. Cells were then observed with a Leica SP5 acousto optical beam splitter confocal laser scanning microscope (Leica Microsystems, GmbH Wetzlar, Germany) and analysed using Leica Application Suite Advanced Fluorescence Lite software.

(h) Reactive oxygen species detection assay

Intracellular ROS was measured by the oxidation of DCFH-DA, a non-polar cell-penetrating molecule, which is hydrolysed by the intracellular esterases to 2′,7′-dichlorodihydrofluorescein and upon oxidation by ROS is oxidized to the fluorophore dichlorofluorescein (DCF) [37]. The

HeLa cells treated with **2**, **4** or the appropriate controls (20μM), following photo-irradiation with visible light (400–700 nm, 10 J cm^{-2}), were washed with PBS under strictly dark conditions, incubated with 10 μM DCFH-DA in PBS for 20 min, washed and overlaid with DMEM/10 per cent FBS medium in the dark. DCF levels were assessed by fluorescence microscopy directly after sample processing, using 485/20 nm excitation and 535/40 nm emission filters.

3. Results and discussion

(a) Design, synthesis and general aspects

We have designed iron-based tumour-targeting biotin conjugates as photocytotoxins that are likely to be internalized in cells by the SMVTs. The photosensitizer is an iron(III) complex in which the biotin unit is covalently linked to the phenazine moiety (see the electronic supplementary material, schemes S1 and S2). The biotin conjugate is expected to accumulate more in the SMVTs overexpressing cancer cells and should have lesser accumulation in the non-cancerous cells. The conjugate on photo-excitation with a light of suitable wavelength should kill the photoexposed cancer cells. The dosage required to elicit photocytotoxic response would be less, thus reducing any side effects. The ligand dppzNB obtained from conjugation of dppza by amide coupling with biotin acyl chloride in DMF is chosen for our study [26,38]. The ligand dppzCB synthesized by coupling biotinylethylenediamine with dppzc after activation with carbonyldiimidazole in DMF is also used for the present work [39]. The fluorescent probe BFITC is synthesized from the reaction of biotinylethylenediamine with FITC in DMSO.

Iron(III) complexes [Fe^{III}(L)(B)] were prepared from a general synthetic procedure in which the tetradentate phenolate ligand (H_3L) was reacted with $Fe(NO_3)_3 \cdot 9H_2O$ in the presence of triethylamine and the dipyridophenazine derivatives (B: dppzNB in **2**; dppzCB in **4**) (scheme 1). The physico-chemical data for the complexes are given in table 1. The complexes are discrete monomeric non-electrolytic species. They are stable in the solution phase as evidenced from the mass spectral data in MeOH showing essentially the molecular ion peak (see the electronic supplementary material, figures S1 and S2). The complexes show characteristic IR spectral features for the amide moiety in the complexes. The electronic absorption spectral profiles of the complexes, shown in figure 1 for complex **2**, are similar to that of their parent complexes **1** and **3** with minor red shift of the ligand centered bands above 400 nm for **2** and below 400 nm for **4** (see the electronic supplementary material, figures S3 and S4) [26]. The broad absorption tail of the phenolate to iron(III) charge transfer band is retained in the complexes, and this allows us to use low-energy visible light for photocytotoxicity study [41]. The solution phase magnetic susceptibility measurements of the complexes in DMSO-d_6 at 25°C gave a magnetic moment value between 5.95 and 6.01 μ_B, corresponding to five unpaired electrons suggesting the high-spin nature of the $3d^5$-iron(III) complexes. The complexes are redox active. Cyclic voltammetric measurements showed a response near −0.68 V (versus SCE) in DMF–0.1 M TBAP, which is assignable to the Fe(III)–Fe(II) redox couple (see figure 1 and electronic supplementary material, figures S5 and S6). Complexes **2** and **4** displayed a quasi-reversible cyclic voltammetric response near 1.1 V, which could involve the biotin sulfur moiety.

(b) DNA binding

The binding behaviour of the complexes to DNA was studied using different methods such as absorption, emission and DNA thermal denaturation (see the electronic supplementary material, table S1). The absorption spectral technique is used to determine the intrinsic binding constant (K_b) value of the complex to the ct-DNA by monitoring the absorption intensity of the charge transfer spectral band of the complex near 300 nm with increasing concentration of DNA keeping the complex concentration as constant. No significant spectral changes were observed with increasing concentrations of ct-DNA. This could be owing to low DNA-binding strength of the complexes **2** and **4**. Relative binding strength of the ternary iron(III) complexes to ct-DNA was

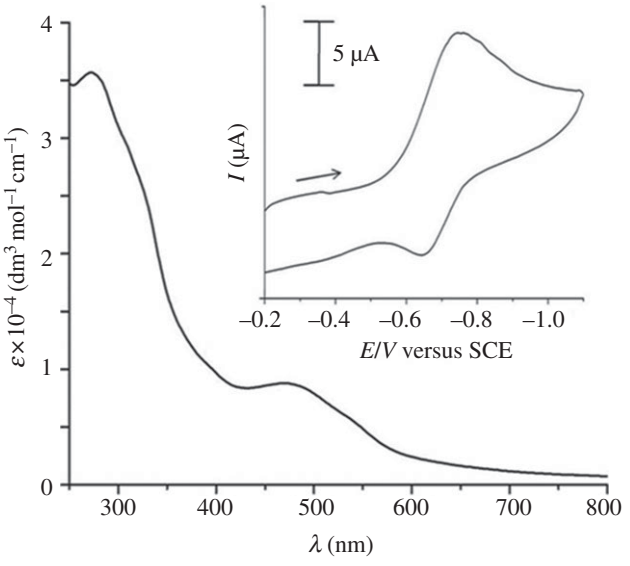

Figure 1. Electronic absorption spectrum of complex **2** in 6% DMF–Tris–HCl buffer. The inset shows the cyclic voltammogram of the Fe(III)–Fe(II) redox couple of complex **4** in DMF–0.1 M TBAP at a scan rate of 50 mV s^{-1}.

Table 1. Selected physico-chemical data for the complexes **2** and **4**.

complex	λ/nm (ε/dm^3 mol^{-1} cm^{-1})[a]	E_f/V (ΔE_p/mV)[b]	Λ_M/Sm^2 mol^{-1}[c]	μ_{eff}[d]	ESI-MS[e]
2	468 (8770)	−0.67 (60)	15	5.95	1088.5
4	480 (5850)	−0.69 (100)	19	6.01	1159.6

[a]Visible electronic spectral band in 6% DMF–Tris–HCl buffer.
[b]Scan rate of 50 mV s^{-1} in DMF–0.1 M TBAP. The Fe(III)–Fe(II) redox potentials are versus saturated calomel electrode (SCE). $E_f = 0.5(E_{pa} + E_{pc})$ and $\Delta E_p = (E_{pa} - E_{pc})$, where E_{pa} and E_{pc} are the anodic and cathodic peak potentials, respectively.
[c]Λ_M, molar conductivity in DMF at 25°C.
[d]μ_{eff} in μ_B for DMSO solution of the complexes at 25°C.
[e]Electrospray ionization (ESI) mass spectra of the complexes in MeOH. The data for $[M + H^+]$.

Table 2. Photocytotoxicity of the iron(III) complexes **1**–**4** and cisplatin in HepG2, HeLa and HEK293 cells.

	HepG2		HeLa		HEK293	
	IC_{50} value/μM		IC_{50} value/μM		IC_{50} value/μM	
complex	dark	light[a]	dark	light[a]	dark	light[a]
[FeL(dppza)] (**1**)[b]	18.7 ± 2.4	10.3 ± 1.8	—	—	—	—
[FeL(dppzNB)] (**2**)	48.8 ± 4.3	5.1 ± 0.8	81.9 ± 5.4	14.5 ± 2.7	59.3 ± 3.3	19.2 ± 1.9
[FeL(dppzc)] (**3**)[b]	—	—				
[FeL(dppzCB)] (**4**)[b]	15.1 ± 1.4	7.8 ± 1.1	—	—	—	—
Cisplatin[c]	32.1[c]	—	—	—	—	—

[a]Photoreactor light of 400–700 nm, power of 10 J cm^{-2}.
[b]Not measured for HeLa and HEK293 cells for complexes **1**, **4** and cisplatin. Not measured for the HepG2 cells for complex **3**.
[c]Data from [40].

obtained by emission spectroscopy from competitive binding assay using EB bound DNA (see the electronic supplementary material, figure S7) [42–44]. EB is non-emissive in Tris-buffer medium owing to solvent quenching of free EB by the solvent molecules [45]. In the presence of DNA, EB showed enhanced emission intensity owing to its intercalative binding to DNA. A competitive binding of the iron(III) complexes to DNA could result in the release of the DNA-bound EB to the aqueous medium, thus resulting in a decrease in its emission intensity. The emission titration data showed that the biotin-conjugated iron(III) complexes are weak binders to DNA. Thermal behaviour of ct-DNA in the presence of the metal complexes gives an insight into the conformational changes and information about the interaction strength of the complexes with the DNA [46]. Thermal denaturation experiments showed only insignificant changes in the DNA melting temperature giving ΔT_m values of -0.15 to 0.3°C, suggesting surface binding interaction of the complexes with the DNA (see the electronic supplementary material, figure S8).

(c) Proteinase K assay

Proteinase K assay was conducted to understand whether the amide bond present in the ligands dppzNB and dppzCB are susceptible to cleavage by intracellular proteases, leading to the release of the dppz ligands and biotin (see the electronic supplementary material, figures S9 and S10). Proteinase K (also protease K or endopeptidase K) is a serine protease with broad substrate specificity [47]. Incubation of the dppzNB ligand with proteinase K for 4 h at 37°C and analysis of the products generated by mass spectrometry showed that the amide bond in dppzNB undergoes digestion (see the electronic supplementary material, figure S9). The dppzCB ligand also showed cleavage, but the site of cleavage is the biotin-ethylenediamine amide bond rather than the dppz-ethylenediamine amide bond. This could be owing to the substrate specificity of proteinase K, which cleaves the peptide bonds more efficiently when the carboxylate group is attached to an alkyl chain. These results indicate that the amide bond is susceptible to undergo digestion by the intracellular proteases, leading to the release of the photoactive iron(III) complex and the targeting moiety, i.e. biotin. Such proteolytic activation of drugs has been widely applied in cancer prodrug designing [48–50].

(d) Cell cytotoxicity

Photocytotoxicity studies with the iron(III) complexes **1**, **2** and **4** were carried out in HepG2, HeLa and HEK293 cells upon irradiation with a broadband visible light source (400–700 nm, 10 J cm^{-2}), and the cell viability was assessed using the MTT assay (table 2). The choice of three different cell lines for this study is based on the facts that (i) hepatocyte HepG2 cells overexpress SMVTs depending on biotin availability, (ii) HeLa cells present highly proliferative growth models usually found in cancerous tissues, and (iii) HEK293 represents a transformed non-cancerous cell line, which possesses SMVTs similar to normal cells. Although most of the cancer cells are well known to possess overexpressed SMVTs, enterocytes (representative cell line, Caco-2) and hepatocytes are largely involved in biotin uptake and regulation [51]. Complex **2** showed a dose-dependent decrease in cell viability in the HepG2 cells with an IC_{50} value of 5.1 μM upon pre-incubation of the complex with the cells for 12 h in the dark followed by photoexposure with visible light (figure 2). The cells that were treated with complex **2** but unexposed to light gave an IC_{50} value of 48.8 μM, indicating significantly low dark toxicity. Control experiments carried out with $Fe(NO_3)_3 \cdot 9H_2O$ or light (400–700 nm) alone showed no significant effects on cell viability in HepG2 cells, thus excluding any possible toxic effects of the components individually (see the electronic supplementary material, figure S11). A time-dependent study was carried out with complex **2** (6 μM) for different pre-incubation periods of 1, 4, 8, 12 and 16 h. It was observed that short pre-incubation (1 and 4 h) of the HepG2 cells with complex **2** followed by photoexposure did not have any significant effect on the cell viability. On pre-incubation for 8 h, the cell viability decreased and upon incubation for an additional 4 h, significant change in cell viability was found after photoexposure. To see whether further incubation decreases the cell viability, incubation

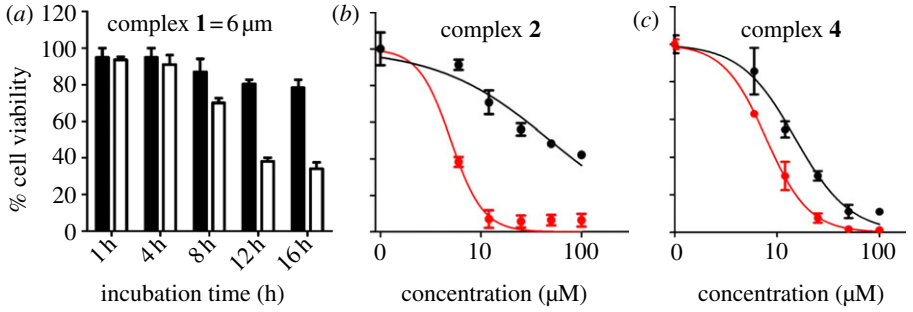

Figure 2. (*a*) Photocytotoxicity of complex **2** (6 μM) in HepG2 cells for various pre-incubation times followed by photoexposure to visible light (400–700 nm, 10 J cm^{-2}) as determined by the MTT assay. The black bars represent cells unexposed to light and the white bars represent cells treated with visible light. Photocytotoxicity of (*b*) complex **2** and (*c*) complex **4** in HepG2 cells on 12 h pre-incubation followed by photoexposure to visible light (400–700 nm, 10 J cm^{-2}) as determined by the MTT assay. Black circles denote cells treated with the complexes but unexposed to light. Grey (red) circles denote cells treated with the complexes and exposed to visible light. (Online version in colour.)

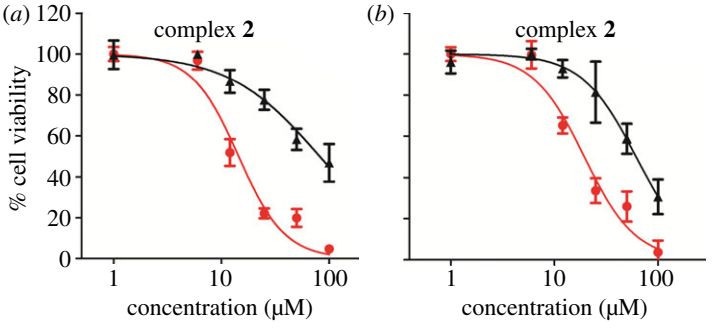

Figure 3. Photocytotoxicity of complex **2** in (*a*) HeLa and (*b*) HEK293 cells on 12 h pre-incubation followed by photoexposure to visible light (400–700 nm, 10 J cm^{-2}) as determined by the MTT assay. Black triangles denote cells treated with the complex but unexposed to light. Grey (red) circles denote cells treated with the complex and exposed to visible light. (Online version in colour.)

with complex **2** was carried out for 16 h in the dark followed by photoexposure to visible light. The cell viability measurements showed an insignificant improvement in the photocytotoxic potential of the complex. Therefore, we carried out the photocytotoxicity measurements with the complexes with a pre-incubation time of 12 h prior to photoexposure to a visible light. This observation might be owing to a slow growth rate of the HepG2 cells or it might result from the biotin-induced expression of SMVTs.

Photocytotoxicity studies with complex **4** in HepG2 cells showed that it becomes toxic to the HepG2 cells in the dark on incubation for 12h, giving an IC_{50} value of 15.1 μM (figure 2). Upon photoexposure, nearly twofold increases in cytotoxicity were observed, giving an IC_{50} value of 7.8 μM. We also investigated the photocytotoxicity of the parent complex **1** in HepG2 cells. It was observed that complex **1** behaves as a cytotoxin with an IC_{50} value of 18.7 μM with approximately 1.8-fold enhancement upon photoexposure to visible light of 400–700 nm ($IC_{50} = 10.3$ μM).

Further photocytotoxicity studies were carried out on HeLa and HEK293 cell lines using complex **2** (figure 3). The HeLa cells on pre-incubation with the complex for 12 h in the dark and subsequent phototreatment showed significant photocytotoxicity to the cells with an IC_{50} value of 14.5 μM in the light and an IC_{50} value of 81.9 μM in the dark. Cell viability measurements on HEK293 cells showed that the complex is photocytotoxic in HEK293 cells with IC_{50} values of 19.2 μM in the light and 59.3 μM in the dark. The photocytotoxic potential of complex **2** varies

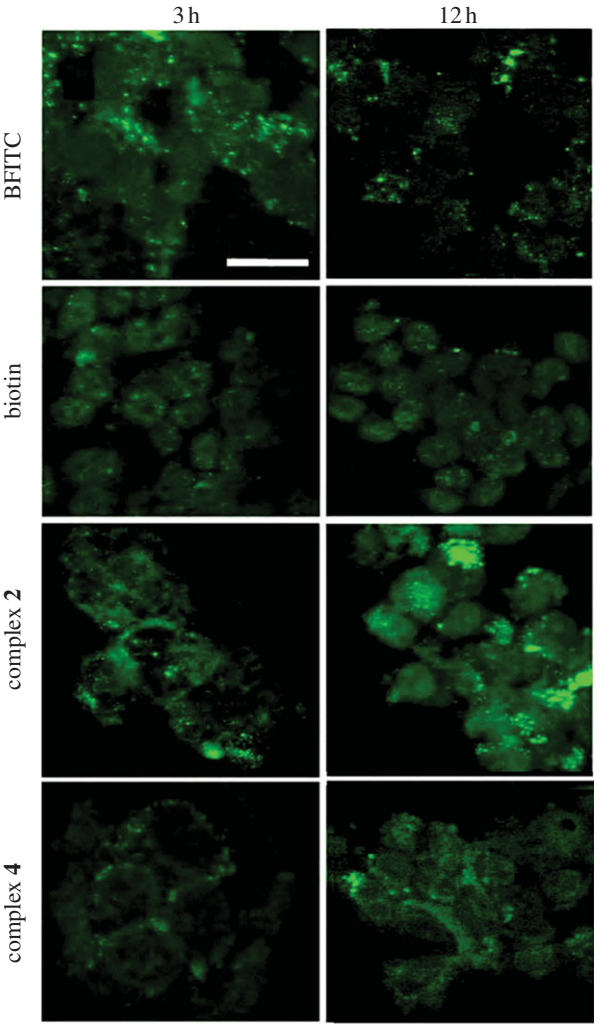

Figure 4. Cellular uptake of biotin (10 nM), BFITC (10 nM), complexes **2** and **4** (20 μM) in HepG2 cells as observed by confocal microscopy with 488 nm excitation and 520 nm emission. Biotin, complexes **2** and **4** required staining with FITC-conjugated streptavidin for detection. Scale bar, 50 μm.

from one cell type to another. This effect could only be rationalized by the presence of biotin transporters in the HepG2 cells over HeLa or HEK293 cells. A nearly threefold enhancement in photocytotoxic potential was observed on going from HeLa cells to HepG2 cells, whereas a 3.7-fold enhancement was observed on going from HEK293 cells to HepG2 cells. The higher photocytotoxicity in HeLa could be a consequence of its high proliferation rate, whereas in the case of HEK293, the SMVT content is significantly low. It should be noted that HeLa cells do express the SMVTs and have been employed in the study of biotin-mediated targeting [52]. It is observed that cytotoxicity of **2** and **4** upon photo-irradiation is significantly higher than that of cisplatin in HepG2 cells (table 2) [40].

(e) Cellular internalization

Cellular uptake of small molecules takes place mainly by endocytosis and/or passive diffusion. Biotin and biotin derivatives are internalized in cells by an active transport process with the involvement of SMVTs [53]. Internalization of native biotin, the fluorescent probe BFITC and complexes **2** and **4** was monitored by confocal fluorescence microscopy in HepG2 and HEK293

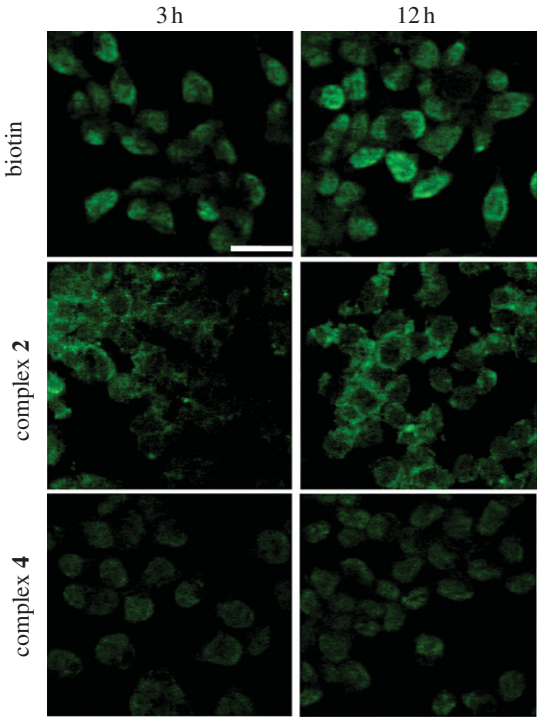

Figure 5. Cellular uptake of biotin (10 nM), complexes **2** and **4** (20 μM) as observed by confocal microscopy in HEK293 cells with 488 nm excitation and 520 nm emission. Biotin, complexes **2** and **4** required staining with FITC-conjugated streptavidin for detection. Scale bar, 40 μm.

cells (figures 4 and 5). The HepG2 cells after incubation for 3 h with native biotin were found to be internalized through a receptor-mediated endocytosis (RME) process that is apparent from the punctated staining as observed after staining with streptavidin–FITC (figure 4). The cells that were incubated with native biotin for 12 h exhibited predominantly nuclear localization of biotin with reduction in cytosolic localization when compared with cells incubated for 3 h with biotin. These observations were further confirmed with the use of fluorescent probe BFITC, which showed similar localization and uptake in the HepG2 cells with the endocytosis mechanism operative as observed after 3 h of incubation. The probe showed that the biotin-conjugate is translocated into the nucleus after 12 h of incubation as observed with the native biotin. The diffuse fluorescence in the cytoplasm observed in all the cases indicates that the primary mode of uptake of biotin is through RME with partial uptake by diffusion. The biotin-conjugated iron(III) complexes **2** and **4** were also investigated for their cellular uptake and localization. Similar to that of native biotin, extensive vesicular uptake of the complexes was observed through streptavidin–FITC staining after 3 h of incubation with the complexes. After 12 h of incubation and concomitant staining with streptavidin–FITC, a largely nuclear localization was observed for the complexes. Again, the cytosolic localization appeared to be in endosomal vesicles, as revealed through punctated staining of the cytosol.

Cellular uptake of native biotin and the complexes **2** and **4** were also monitored in HEK293 cells through streptavidin–FITC staining at time points of 3 and 12 h (figure 5). The HEK293 cell line is a transformed cell line that, unlike HepG2 and HeLa cells, does not express high levels of SMVTs on the cell surface. If this is the case, then native biotin and the biotinylated iron(III) complexes are expected to be taken up only by passive diffusion in the absence of any alternative pathway of RME. Confocal microscopic investigation showed that native biotin is taken up into the HEK293 cells by a diffusion process that is apparent from the diffuse staining of the cytosol after 3 h pretreatment with biotin. Complexes **2** and **4** also exhibited similar features with diffuse

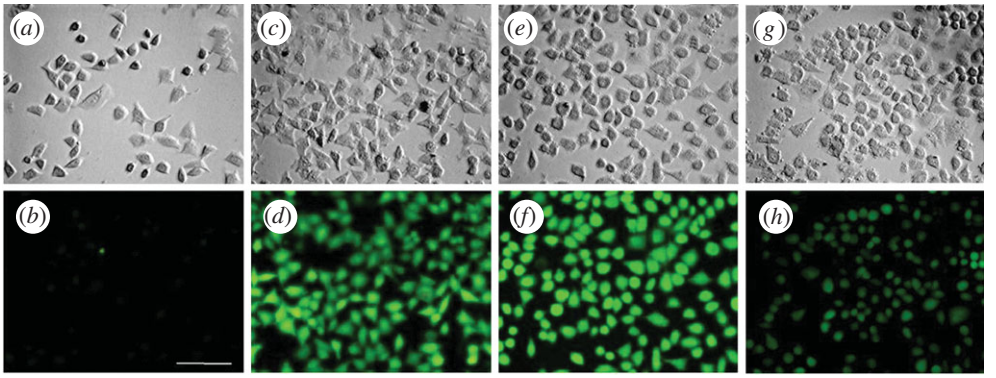

Figure 6. The effect of PDT on oxidation of DCFH-DA (10 μM) to DCF as observed by fluorescence microscopy with 485/20 nm excitation and 535/40 nm emission: (*a*,*b*) without complex **2** (20 μM), (*c*,*d*) with complex **2** (20 μM) for a light dose of 5 J cm^{-2}, (*e*,*f*) with complex **2** (20 μM) for a light dose of 10 J cm^{-2} and (*g*,*h*) with complex **4** (20 μM) for a light dose of 10 J cm^{-2}. The images were acquired 30 min after PDT (following treatment with DCFH-DA for 20 min). Scale bar, 50 μm.

staining of the cytoplasm after 3 h pretreatment with the complexes. After 12 h, complex **2** was found to be mostly localized in the cytosol with moderate staining of the nucleus. Complex **4** was found to be localized equally in cytosol and the nucleus. Taken together, these experiments indicate that the mechanism of cellular uptake of native biotin and biotinylated complexes is largely through RME involving specific vitamin receptors in the HepG2 cells, while the uptake is largely by passive diffusion in HEK293 cells. The cellular internalization data suggest that conjugation of a photoactivable moiety, such as the iron(III) dppz species, to the vitamin does not have any significant effect on the uptake mechanism of the vitamin in the cells.

(f) Reactive oxygen species detection

To determine the species responsible for the observed cell death in HepG2, HeLa and HEK293 cell lines, we carried out a DCF assay in HeLa cells (figure 6). The untreated control cells appeared unstained or very lightly stained, indicating very low levels of ROS or oxidative stress in those cells. The HeLa cells that were treated with both complex **2** and visible light (400–700 nm, 5 J cm^{-2}) showed an increase in the levels of DCF fluorescence when compared with the untreated controls (figure 6*d*). The light dose was increased from 5 to 10 J cm^{-2} to observe the light-dose dependence on ROS generation. It was observed that with an increase in the light dose, the DCF fluorescence intensity became enhanced, and a decrease in the cell size was observed, which can be ascribed to the effect of PDT on the cells (figure 6*f*). This observation was further confirmed from the bright-field images that showed a change in the cell morphology from spindle shaped to circular shaped (figure 6*e*). The DCF assay was carried out with complexes **4** and **5**, which showed a much lower level of ROS upon photo-irradiation with the visible light (10 J cm^{-2}), but rounding up of the cells was observed in the case of cells treated with complex **4** (figure 6*g*,*h*). The data suggest that oxidative stress produced inside the cells owing to photo-induced ROS generation by the complexes could be largely responsible for the observed cell death.

4. Conclusions

This work reports two new iron(III) complexes of a tetradentate phenolate-based ligand and the biotin-conjugated dipyridophenazine derivatives that were designed and synthesized for targeted delivery of the photocytotoxic complexes specifically to tumour tissues, and to reduce their accumulation in normal non-malignant tissue. The biotin-appended iron(III) complexes showed no aparent loss in activity in streptavidin-binding assay, but the tumour-targeting moiety lost its ability to interact favourably with DNA. Selective photocytotoxicity in hepatocellular

carcinoma cell lines over normal immortilized cells was observed, indicative of selective uptake in the HepG2 cells. Fluorescence microscopic studies established that a significantly different uptake pathway was operative in HepG2 cells compared with HEK293 cells. This work shows that through suitable designing, three-dimensional metal-based PDT agents of bio-essential metal ions such as iron can be specifically delivered to tumour tissue, thus minimizing side effects in non-cancerous tissue caused by their accumulation. This study further established the fact that a double selectivity could be achieved by coupling cancer-specific targeting moiety and a metal-based PDT agent for effective cancer management and cure. Additional studies warrant the evaluation of these complexes with SMVT genes transfected into HEK293 cells and observing the photocytotoxic effects therein. A different approach could be knock-down of SMVT genes by shRNA in HepG2 cells and to look whether it leads to a reduction in phototoxic potential. Moreover, an *in vivo* study on mouse xenograft models of hepatocellular carcinoma is expected to give a more rigorous evaluation of the tumour targeting approach.

We thank the Department of Science and Technology (DST), Government of India, for financial support (SR/S5/MBD-02/2007) and IRIS and SID of IISc for microscopy facilities. We are grateful to the Alexander von Humboldt Foundation, Germany, for an electrochemical system. S.S. and A.H. thank CSIR, New Delhi, for research fellowships. A.R.C. thanks DST. for a J. C. Bose National Fellowship.

References

1. Ethirajan M, Chen Y, Joshi P, Pandey RK. 2011 The role of porphyrin chemistry in tumor imaging and photodynamic therapy. *Chem. Soc. Rev.* **40**, 340–362. (doi:10.1039/B915149B)
2. Bonnett R. 2000 *Chemical aspects of photodynamic therapy*. London, UK: Gordon & Breach.
3. Ojima I *et al.* 2002 Tumor-specific novel taxoid-monoclonal antibody conjugates. *J. Med. Chem.* **45**, 5620–5623. (doi:10.1021/jm025540g)
4. Ludwig JA, Weinstein JN. 2005 Biomarkers in cancer staging, prognosis and treatment selection. *Nat. Rev. Cancer* **5**, 845–856. (doi:10.1038/nrc1739)
5. Jaracz S, Chen J, Kuznetsova LV, Ojima I. 2005 Recent advances in tumor-targeting anticancer drug conjugates. *Bioorg. Med. Chem.* **13**, 5043–5045. (doi:10.1016/j.bmc.2005.04.084)
6. Ojima I. 2008 Guided molecular missiles for tumor-targeting chemotherapy—case studies using the second-generation taxoids as warheads. *Acc. Chem. Res.* **41**, 108–119. (doi:10.1021/ar700093f)
7. Chen J, Jaracz S, Zhao X, Chen S, Ojima I. 2005 Antibody–cytotoxic agent conjugates for cancer therapy. *Exp. Opin. Drug Deliv.* **2**, 873–890. (doi:10.1517/17425247.2.5.873)
8. Wu X, Ojima I. 2004 Tumor specific novel taxoid-monoclonal antibody conjugate. *Curr. Med. Chem.* **11**, 429–435. (doi:10.2174/0929867043455963)
9. Hamaan PR *et al.* 2002 Gemtuzumab ozogamicin, a potent and selective Anti-CD33 antibody-calicheamicin conjugate for treatment of acute myeloid leukemia. *Bioconjugate Chem.* **13**, 47–58. (doi:10.1021/bc010021y)
10. Bradley MO *et al.* 2001 Tumor targeting by covalent conjugation of a natural fatty acid to paclitaxel. *Clin. Cancer Res.* **7**, 3229–3238.
11. Kuznetsova L, Chen J, Sun L, Wu X, Pepe A, Veith JM, Pera P, Bernacki RJ, Ojima I. 2006 Syntheses and evaluation of novel fatty acid-second-generation taxoid conjugates as promising anticancer agents. *Bioorg. Med. Chem. Lett.* **16**, 974–977. (doi:10.1016/j.bmcl.2005.10.089)
12. Leamon CP, Reddy JA. 2004 Folate-targeted chemotherapy. *Adv. Drug Deliv. Rev.* **56**, 1127–1141. (doi:10.1016/j.addr.2004.01.008)
13. Lu Y, Low PS. 2002 Folate-mediated delivery of macromolecular anticancer therapeutic agents. *Adv. Drug Deliv. Rev.* **54**, 675–693. (doi:10.1016/S0169-409X(02)00042-X)
14. Lee JW, Lu JY, Low PS, Fuchs PL. 2002 Synthesis and evaluation of taxol–folic acid conjugates as targeted antineoplastics. *Bioorg. Med. Chem.* **10**, 2397–2406. (doi:10.1016/S0968-0896(02)00019-6)
15. Chu TC, Marks III JW, Lavery LA, Faulkner S, Rosenblum MG, Ellington AD, Levy M. 2006 Aptamer: toxin conjugates that specifically target prostate tumor cells. *Cancer Res.* **66**, 5989–5992. (doi:10.1158/0008-5472)

16. Farokhzad OC, Cheng J, Teply BA, Sherifi I, Jon S, Kantoff PW, Richie JP, Langer R. 2006 Targeted nanoparticle-aptamer bioconjugates for cancer chemotherapy *in vivo*. *Proc. Natl Acad. Sci. USA* **103**, 6315–6320. (doi:10.1073/pnas.0601755103)
17. Nakanishi T, Tamai I, Takaki A, Tsuji A. 2000 Cancer cell-targeted drug delivery utilizing oligopeptide transport activity. *Int. J. Cancer* **88**, 274–280. (doi:10.1002/1097-0215(20001015)88:2<274::AID-IJC20>3.0.CO;2-5)
18. Nagy A *et al.* 1998 Synthesis and biological evaluation of cytotoxic analogs of somatostatin containing doxorubicin or its intensely potent derivative,2-pyrrolinodoxorubicin. *Proc. Natl Acad. Sci. USA* **95**, 1794–1799. (doi:10.1073/pnas.0610763104)
19. Luo Y, Bernshaw NJ, Lu Z-R, Kopecek J, Prestwich GD. 2002 Targeted delivery of doxorubicin by HPMA copolymer-hyaluronan bioconjugates. *Pharm. Res.* **19**, 396–400. (doi:10.1023/A:1015170907274)
20. Russell-Jones G, McTavish K, McEwan J, Rice J, Nowotnik D. 2004 Vitamin-mediated targeting as a potential mechanism to increase drug uptake by tumours. *J. Inorg. Biochem.* **98**, 1625–1633. (doi:10.1016/j.jinorgbio.2004.07.009)
21. Reddy JA, Westrick E, Vlahov I, Howard SJ, Santhapuram HK, Leamon CP. 2006 Folate receptor specific anti-tumor activity of folate-mitomycin conjugates. *Cancer Chemother. Pharmacol.* **58**, 229–236. (doi:10.1007/s00280-005-0151-z)
22. Liu Z, Zhong Z, Peng G, Wang S, Du X, Yan D, Zhang Z, He Q, Liu J. 2009 Folate receptor mediated intracellular gene delivery using the charge changing solid lipid nanoparticles. *Drug Deliv.* **16**, 341–347. (doi:10.1080/10717540903047387)
23. Leamon CP, Reddy JA, Vlahov IR, Vetzel M, Parker N, Nicoson JS, Xu L-C, Westrick E. 2005 Synthesis and biological evaluation of EC72: a new folate-targeted chemotherapeutic. *Bioconjugate Chem.* **16**, 803–811. (doi:10.1021/bc049709b)
24. Chen S, Zhao X, Chen J, Chen J, Kuznetsova L, Wong SS, Ojima I. 2010 Mechanism-based tumor-targeting drug delivery system. Validation of efficient vitamin receptor-mediated endocytosis and drug release. *Bioconjug. Chem.* **21**, 979–987. (doi:10.1021/bc9005656)
25. Saha S, Majumdar R, Roy M, Dighe RR, Chakravarty AR. 2009 An iron complex of dipyridophenazine as a potent photocytotoxic agent in visible light. *Inorg. Chem.* **48**, 2652–2663. (doi:10.1021/ic8022612)
26. Saha S, Mallick D, Majumdar R, Roy M, Dighe RR, Chakravarty AR. 2011 Structure-activity relationship of photocytotoxic iron(III) complexes of modified dipyridophenazine ligands. *Inorg. Chem.* **50**, 2975–2987. (doi:10.1021/ic1024229)
27. Perrin DD, Armarego WLF, Perrin DR. 1980 *Purification of laboratory chemicals*. Oxford, UK: Pergamon Press.
28. Wilson JG. 1990 Phenolic analogs of amino carboxylic acid ligands for ^{99m}Tc. 4. N-(2-Hydroxybenzyl) glycines (hbg). *Aust. J. Chem.* **43**, 1283–1289. (doi:10.1071/CH9901283)
29. Evans DF. 1959 The determination of the paramagnetic susceptibility of substances in solution by nuclear magnetic resonance. *J. Chem. Soc.* 2003–2005. (doi:10.1039/JR9590002003)
30. Evans DF, James TA. 1979 Variable-temperature magnetic-susceptibility measurements of spin equilibria for iron(III) dithiocarbamates in solution. *J. Chem. Soc. Dalton Trans.* 723–726. (doi:10.1039/DT9790000723)
31. Green NM. 1970 Spectrophotometric determination of avidin and biotin. *Methods Enzymol.* **18A**, 418–424. (doi:10.1016/0076-6879(71)18342-5)
32. Reichman ME, Rice SA, Thomas CA, Doty P. 1954 A further examination of the molecular weight and size of desoxypentose nucleic acid. *J. Am. Chem. Soc.* **76**, 3047–3053. (doi:10.1021/ja01640a067)
33. McGhee JD, von Hippel PH. 1974 Theoretical aspects of DNA-protein interactions: co-operative and non-co-operative binding of large ligands to a one-dimensional homogeneous lattice. *J. Mol. Biol.* **86**, 469–489. (doi:1016/0022-2836(74)90031-X)
34. Carter MT, Rodriguez M, Bard AJ. 1989 Voltammetric studies of the interaction of metal chelates with DNA. 2. Tris-chelated complexes of cobalt(III) and iron(II) with 1,10-phenanthroline and 2,2′-bipyridine. *J. Am. Chem. Soc.* **111**, 8901–8911. (doi:10.1021/ja00206a020)
35. Freimoser FM, Jakob CA, Aebi M, Tuor U. 1999 The MTT [3-(4,5-dimethylthiazol-2-yl)-2,5-diphenyltetrazolium bromide] assay is a fast and reliable method for colorimetric determination of fungal cell densities. *Appl. Environ. Microbiol.* **65**, 3727–3729.

36. Iinuma S, Farshi SS, Ortel B, Hasan T. 1994 A mechanistic study of cellular photodestruction with 5-aminolaevulinic acid-induced porphyrin. *Br. J. Cancer,* **70**, 21–28. (doi:10.1038/bjc.1994.244)
37. Le Bel CP, Ischiropoulos H, Bondy SC. 1992 Evaluation of the probe 2′,7′-dichlorofluorescin as an indicator of reactive oxygen species formation and oxidative stress. *Chem. Res. Toxicol.* **5**, 227–231. (doi:10.1021/tx00026a012)
38. Slim M, Durisic N, Grutter P, Sleiman HF. 2007 DNA–protein noncovalent cross-linking: ruthenium dipyridophenazine biotin complex for the assembly of proteins and gold nanoparticles on DNA templates. *ChemBioChem* **8**, 804–812. (doi:10.1002/cbic.200600550)
39. Lo KK-W, Chung C-K, Zhu N. 2006 Nucleic acid intercalators and avidin probes derived from luminescent cyclometalated iridium(III)-dipyridoquinoxaline and -dipyridophenazine complexes. *Chem. Eur. J.* **12**, 1500–1512. (doi:10.1002/chem.200500885)
40. Lu Y-H, Tang C, Wang W, Xi T. 2009 Down regulation of surviving gene and upregulation of p53 gene expression by siRNA induces apoptosis in human hepatocellular carcinoma cell line HepG2. *J. Biomed. Sci. Eng.* **2**, 57–62. (doi:10.4236/jbise.2009.21010)
41. Ramaiah D, Eckert I, Arun KT, Weidenfeller L, Epe B. 2002 Squaraine dyes for photodynamic therapy: study of their cytotoxicity and genotoxicity in bacteria and mammalian cells. *Photochem. Photobiol.* **76**, 672–677. (doi:10.1562/0031-8655(2002)076<0672:SDFPTS>2.0.CO;2)
42. Yang X-L, Kaenzig C, Lee M, Wang AH-J. 1999 Binding of AR-1-144, a tri-imidazole DNA minor groove binder, to CCGG sequence analyzed by NMR spectroscopy. *Eur. J. Biochem.* **263**, 646–651. (doi:10.1046/j.1432-1327.1999.00515.x)
43. Waring MJ. 1965 Complex formation between ethidium bromide and nucleic acids. *J. Mol. Biol.* **13**, 269–282. (doi:10.1016/S0022-2836(65)80096-1)
44. LePecq J-B, Paoletti C. 1967 A fluorescent complex between ethidium bromide and nucleic acids. *J. Mol. Biol.* **27**, 87–106. (doi:10.1016/0022-2836(67)90353-1)
45. An Y, Liu S-D, Deng S-Y, Ji L-N, Mao Z-W. 2006 Cleavage of double-strand DNA by linear and triangular trinuclear copper complexes. *J. Inorg. Biochem.* **100**, 1586–1593. (doi:10.1016/j.jinorgbio.2006.05.002)
46. Hilz H, Wiegers U, Adamietz P. 1975 Stimulation of proteinase K action by denaturing agents: application to the isolation of nucleic acids and the degradation of 'masked' proteins. *Eur. J. Biochem.* **56**, 103–108. (doi:10.1111/j.1432-1033.1975.tb02211.x)
47. Law B, Tung C-H. 2009 Proteolysis: a biological process adapted in drug delivery, therapy, and imaging. *Bioconjugate Chem.* **20**, 1683–1695. (doi:10.1021/bc800500a)
48. Kratz F, Müller IA, Ryppa C, Warnecke A. 2008 Prodrug strategies in anticancer chemotherapy. *ChemMedChem* **3**, 20–53. (doi:10.1002/cmdc.200700159)
49. Wu W *et al.* 2006 Targeting cell-impermeable prodrug activation to tumor microenvironment eradicates multiple drug-resistant neoplasms. *Cancer Res.* **66**, 970–980. (doi:10.1158/0008-5472)
50. Pacheco-Alvarez D, Solorzano-Vargas RS, Gonzalez-Noriega A, Michalak C, Zempleni J, Leon-Del-Rio A. 2005 Biotin availability regulates expression of the sodium-dependent multivitamin transporter and the rate of biotin uptake in HepG2 cells. *Mol. Genet. Metab.* **85**, 301–307. (doi:10.1016/j.ymgme.2005.04.001)
51. Mahato R, Tai W, Cheng K. 2011 Prodrugs for improving tumor targetability and efficiency. *Adv. Drug. Deliv. Rev.* **63**, 659–670. (doi:10.1016/j.addr.2011.02.002)
52. Luo S, Kansara V, Zhu X, Mandava NK, Pal D, Mitra AK. 2006 Functional characterization of sodium-dependent multivitamin transporter in MDCK-MDR1 cells and its utilization as a target for drug delivery. *Mol. Pharm.* **3**, 329–339. (doi:10.1021/mp0500768)
53. Kansara V, Luo S, Balasubrahmanyam B, Pal D, Mitra AK. 2006 Biotin uptake and cellular translocation in human derived retinoblastoma cell line (Y-79): a role of hSMVT system. *Int. J. Pharm.* **312**, 43–52. (doi:10.1016/j.ijpharm.2005.12.045)